Scientific Journal of Impact Factor (SJIF): 5.71
e-ISSN (O): 2348-4470
p-ISSN (P): 2348-6406
International Journal of Advance Engineering and Research Development
Volume 6, Issue 04, April -2019

Landslide susceptibility assessment and mapping using GIS and Analytic Hierarchy Process (AHP). Case study: Atalanti watershed, Central Greece

[1]Lappas Ioannis, [2]Kallioras Andreas

[1]Dr. Hydrogeologist, Special Secretariat for Water, Department of Protection and Management of Aquatic Environment, Division of Surface and Ground Waters, Amaliados 17 Str., Ambelokipi-Athens, P.C. 11523,

[2]Assistant Professor, National and Technical University of Athens, School of Mining and Metallurgical Engineering, Laboratory of Engineering Geology and Hydrogeology, Heroon Polytechniou 9 Str., Zografou-Athens, P.C. 15780,

Abstract: *A methodology for landslide susceptibility assessment and mapping in a GIS environment through multi-criteria decision analysis (MCDA) is presented. Landslides belong to the severe natural disasters which are often experienced in Greece and have become a significant concern mainly in the mountainous areas. In this paper, the Analytic Hierarchy Process (AHP) was applied with a varied weighted linear approach to identify the landslide potential associated with the terrain aiming at contributing in landslide risk assessment evaluation. The study was focused on landslide susceptibility mapping in Atalanti catchment located in Central Greece, employing spatial analysis of factors influencing the landslide occurrence. GIS is a useful tool for the construction of landslide prediction model and for application in regional planning, risk management and hazard mitigation as well as early warning for the prioritization of efforts to reduce future landslide hazards. In total, twelve dataset layers including slope angle, slope aspect, rainfall, geology-lithology, curvature, elevation, land use, proximity to the rivers, faults and roads, topogragraphic wetness index (TWI) and stream power index (SPI) were selected as the causative factors for the analysis. Digital elevation model (DEM) of 25x25m resolution was used to extract the topographic, geological, geomorphological, hydrological, land use and climatic related landslide causative-instability factors. The final susceptibility score was classified into susceptible rating values based on the factors' importance and the spatially generated layers were assembled to produce the final landslide indexed susceptibility assessment map. According to the map, 30.4% area of the region is moderately susceptible to the occurrence of landslides, 30.0% area is low to moderate, 19.8% is low, 14.3% is moderate to high and only 3.1% is high to very high susceptible to the landslides' occurrences. Validation results and sensitivity analysis based on landslide inventory showed that this model could be used for the prediction of future landslides since almost 81.8% correspond to areas where landslide phenomena were actually took place. Finally, the analysis of the susceptibility modeling showed the high importance of slope, rainfall, geology and tectonics parameters.*

Keywords: *multi-criteria decision analysis; landslides areas assessment; weighted linear approach; landslides occurrences; sensitivity analysis; Atalanti catchment*

1. Introduction

Landslide is a major geohazard that can be triggered by earthquakes, volcanic eruptions or by human-made activities (Carrara, 1983; Dai et al., 2001). Knowledge of the probability and timing of a landslide event as well as its intensity is particularly useful for project control and design for natural and urban planning. Mapping susceptibility to landslides and slope failures is of particular importance as they are one of the most serious natural disasters causing more and more losses in both human lives and infrastructure (Ladas et al., 2007; Sarkar et al., 2004). Landslides are the result of complex interaction among several factors primarily involving geological, geomorphological and hydrometeorological factors. Successful use of new geoinformatics-based technologies is now an important aid to assessing the conditions in a geo-environment that is threatened and/or destroyed. In this context, the possibility of applying qualitative and quantitative methodologies for the mapping of landslide susceptibility in the wider study area is investigated. The main goal is the map production, which band the areas according to the intensity of the expected risk in landslide. A landslide susceptibility map depicts the areas (or area zones) likely to have landslides in the future, associating some of the main factors that contributed to the occurrence of previous recorded landslides of slope failures. Its reliability depends mainly on the quantity and quality of available geographic data, the scale of work and the choice of the appropriate analysis methods (Shahabi et al., 2015; Tazik et al., 2014).

The methods of mapping susceptibility to landslides are based on Geographic Information Systems (GIS) and divided into two groups: qualitative and quantitative. Qualitative methods depend on the knowledge and the experts' opinions and consequently they are accompanied by a high degree of subjectivity. The method of using indicators or parametric maps is subdivided into two approaches: the combination or superposition of index maps and logical analytical models. These two approaches can be described as semi-quantitative as they incorporate the idea of ranking and weighting. Quantitative – statistical methods are based on the numerical expressions of relationships between controllers and the landslide occurrences, including statistical estimation of combinations of factors that led to landslides in the past and then their performance for regions not yet affected by landslides, but show the same background conditions (multivariate statistical analysis methods). The basis of most landslide studies in a regional scale is the construction of a landslide inventory map, the independent factors causing landslides, the applied method to determine the parameters' weights and the final landslide susceptibility map within a GIS environment. These can be used to compute landslide susceptibility maps depicting the spatial probability of slope failures using a wide range of approaches using GIS as an effective tool for managing and manipulating the spatial data. Several researchers (Atkinson et al., 1998; Carrara et al., 1991; 1999; 2003; 2008; Chau et al., 2004; Chung et al., 2003; Gupta et al., 1990; Kumar et al., 2013; Rozos et al., 2010; 2011) have used multi-criteria decision analysis (MCDA) techniques as a spatial analysis with GIS processing tools, from which the most common one is the Analytic Hierarchy Process (AHP) presented by Saaty (1977; 1980; 1990; 2000), a semi-quantitative method to assign weights to the landslide related triggering parameters through a weighted linear combination technique (WLC) to produce landslide susceptibility maps ().

2. Materials and Methods

2.1 Location Area

The Atalanti watershed lies between $21^0 44'$-$24^0 39$ longitudes and $37^0 45$-$39^0 29'$ latitudes at Lokrida province (Lokri municipality) covering an area of approximately 248 km^2 and perimeter of 105 km in Eastern-Central Greece (Fig.1). The drainage basin has flat relief in lowlands with gentle slopes up to 20^0 (~85%) and steeper ones in highlands with slopes up to 55^0 (~3%). The study area is washed by the sea at the East surrounded by hilly and mountainous ranges such as Mt. Chlomo (Lappas, 2018) forming a quite complex geomorphology. Also, the catchment's elevation begins from the sea level ending up to 1073 m (a.s.l.) crossed by dense and well developed, dendritic to sub-dendritic drainage network with several kilometers of length discharging into Aegean Sea. The flat and hilly terrain covers 76% of the whole basin area mostly concerning the coastal areas while the rest 24% belongs to mountainous areas. Moreover, within Atalanti watershed, there are only seasonal streams, namely, Alargino, Karagkiozis (4th order by Strahler) and Ag. Ioannis (3rd order by Strahler) flowing during winter and spring and form typical V-shape rejuvenated valleys as a result of the intensively active tectonics. Within the southern mountainous range one can observe streams with very steep slopes and deep river bed, especially when carbonate rocks prevail. Finally, the regional area is characterized by mild wet winters and hot, dry summers (typical Mediterranean climate with C_{sa} type according to Köppen classification) with the mean annual precipitation and the air temperature equals to 819.1 mm and 16.8^0C respectively (Lappas, 2018). Almost 75% of the total rainfall takes place in the wet season from October to April with significantly rainfall non-uniformity between the lowlands and highlands.

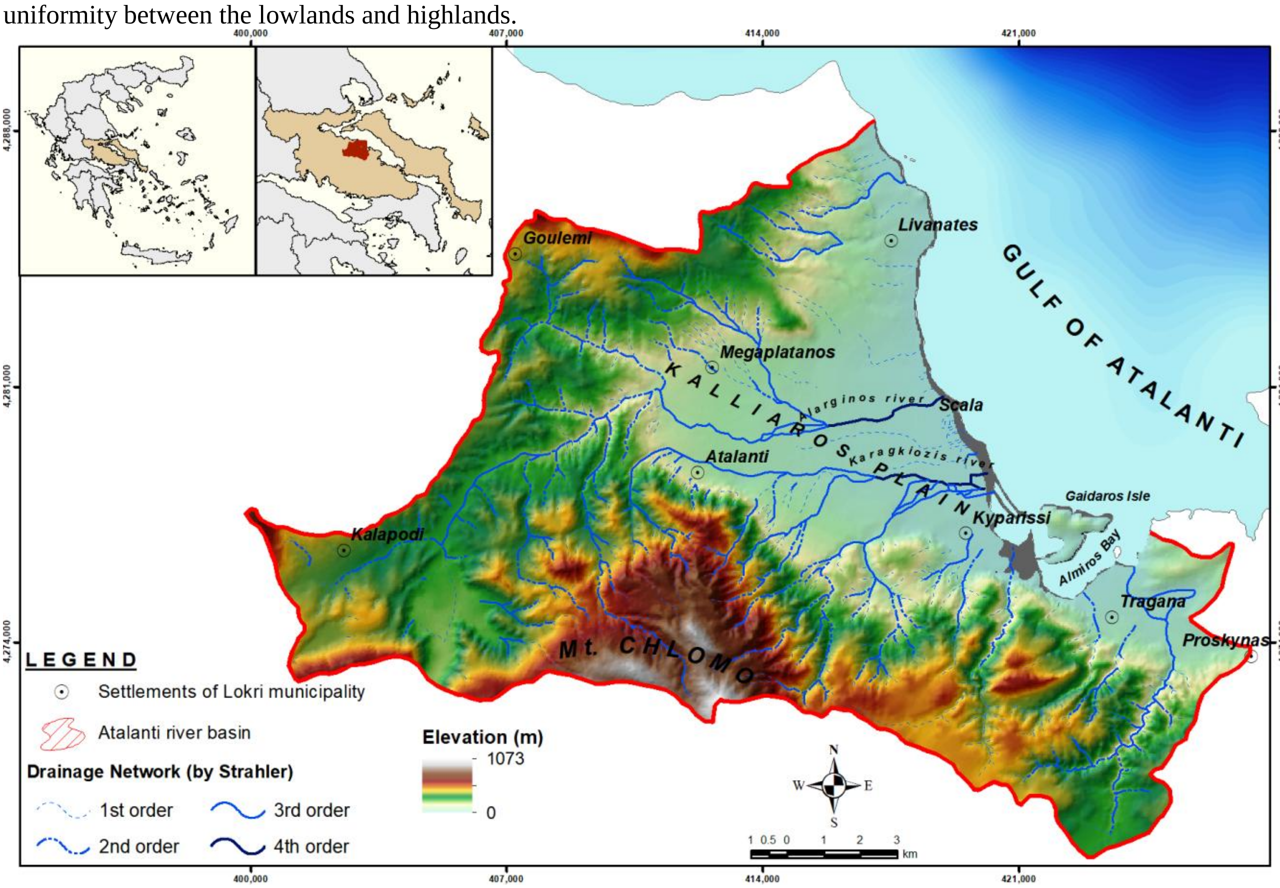

Fig.1: The Atalanti watershed location and geomorphology with its contributing drainage network.

2.2 Input Data

The geo-referenced in GGRS 87 coordinating system topographic maps of 20m and 4m interval (scale from 1:5.000 to 1:50,000) were obtained from the Hellenic Military Geographical Service (HMGS) where the drainage network of the Atalanti watershed is also delineated. According to the aforementioned maps the DEM of 25m grid cell resolution was derived and several calculations were also determined such as the slope, the aspect, the topographic zones as well as the distances to faulting zones, transportation and drainage. Moreover, the geological maps from the regional area of interest (scale 1:50.000) were obtained from the Institute of Geology and Mineral Exploration (IGME) to geologically and tectonically characterize the formations concerning their contribution to landslides (Maratos et al., 1965). Furthermore, monthly and annual rainfall dataset for a large time period (1981-2014) from 35 meteorological and rain gauge stations covering the regional area were obtained from the Hellenic National Meteorological Service (HNMS) and the Ministry of Environment and Energy. Especially, monthly precipitation data from 1963 to 2014 were used from the Atalanti rain gauge station within the river basin under research. Rainfall data within and around the catchment area were finally used to process rainfall factors at each station and then these point data were spatially interpolated to each raster cell in the study area. Also, through CORINE Land Cover (2012), the study area's land use was identified and classified according to landslide susceptibility. All the aforementioned base and derived thematic spatial maps were pre-processed, analyzed and integrated together in a raster GIS environment transformed into a grid spatial database and classified into seven classes on the basis of theirs effect on landslides to display spatial information in order to identify the landslide prone areas. At the end, historical recorded landslides occurrences (19) were used to validate the results based on the landslide inventory database of the Institute of Geology and Mineral Exploration (IGME).

2.3 Methodology Analysis

A semi-quantitative index-based model was selected and developed in a GIS geo-processing environment defining landslide susceptibility areas through the weighting for expressing each criterion's importance to other criteria. The Multi-Criteria Decision Analysis (MCDA) process was performed in order to determine the landslide causative factors analyzing a series of alternatives with a view to ranking them from the most preferable to the least preferable (expert judgement). This was applied by the pairwise comparison method through Analytic Hierarchy Process (AHP) (Saaty, 1977; 1980; 1990; 2000; Saaty et al., 1991). Landslide Susceptibility Index (LSI) consisted, as mentioned before, of twelve independent variables, namely, the basin's slope (in degrees) (S), the aspect-slope direction (A), the curvature (C), the elevation-topographic zones (E), the geology-lithology (G), the rainfall (R), the land use (LU), the distance to tectonics-faulting zones (T), the distance to drainage network (D), the distance to transportation (TR), the topographic wetness index (TWI) and the stream power index (SPI). The selection of these parameters was actually based on their relevance to landslide occurrences as reviewed in the scientific references (Bathrellos et al., 2009; Chalkias et al., 2014; Ferentinou et al., 2010; Kritikos et al., 2011; Mancini et al., 2010; Marinoni, 2004; Papadakis et al., 2017; Polykretis et al., 2014; Tsangaratos et al., 2013). Each parameter was spatially visualized in a thematic map after having been processed in a GIS environment using a weighted overlay analysis and was categorized into seven classes from "Very Low" to "Very High". Following the methodology flowchart (Fig.2), the final LSI was determined using the following equation:

$$LSI = \sum_{i=1}^{n} w_i \cdot R_i$$

where,

R_i *the ranking of each variable*
w_i *the variable's weight assignment*
n *the number of variables (12)*

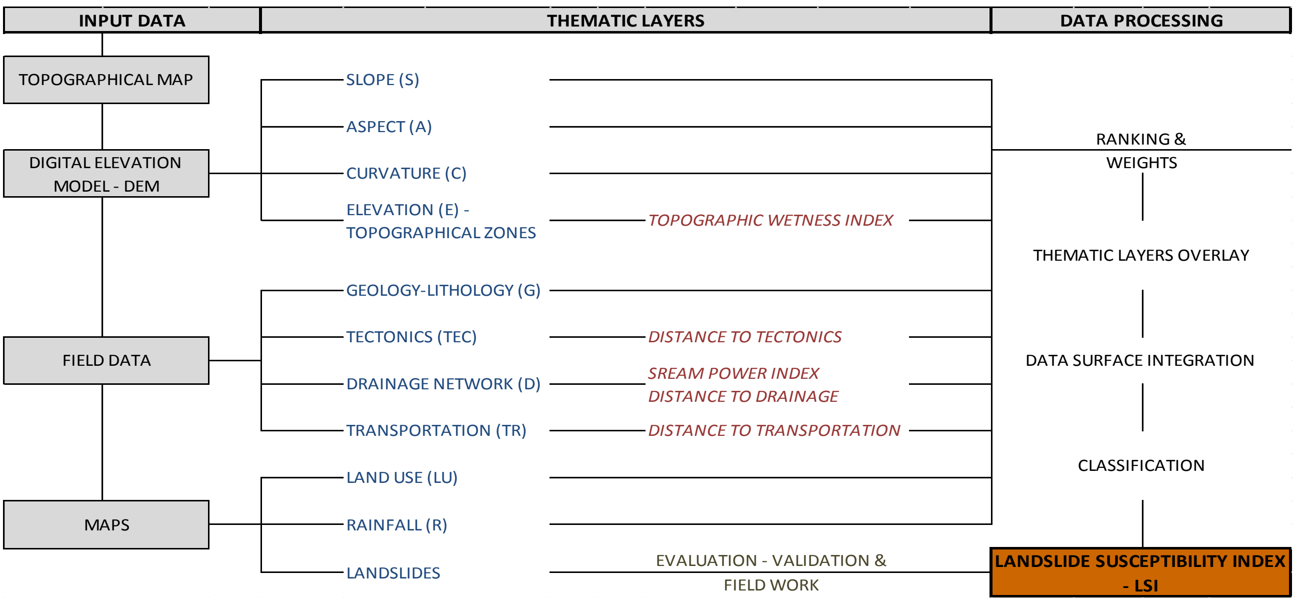

Fig.2: Methodology flowchart.

This AHP method lets us detect the landslide susceptibility areas by identifying the most landslide significant criteria based on the decision makers' preferences being capable of converting subjective assessments of relative importance into a weighted-linear scale transform. This approach was used for comparing each factor map and determining the factor weight values. Furthermore, the criterion pairwise comparison matrix (12×12) takes the pairwise comparisons as an input and produces the relative weighting factors allowing the comparison of two criteria at a time. The relative significance between the criteria is evaluated along the row from 1 to 9 indicating less important to much more important criteria, respectively whereas the reciprocal of the weight (from 1/2 to 1/9) is assigned to the corresponding column (Table 1). Each parameter was assigned a value in a scale between 1 and 10 (rating score) and ranked based on the expert's consultation, knowledge, experience and subjectiveness. The more precise is the judgement the more compatible is the produced map with reality. All the variables are getting prepared separately and are finally assembled to produce the Landslide Susceptibility map.

Table 1: Scale for comparison (by Saaty).

Scale	Deg.of preference	Explanation
1	Equal	Two activities contribute equally
3	Moderate	Experience and judgment slightly to moderately favour one activity over another
5	Strong	Experience and judgment strongly or essentially favour one activity over another
7	Very strong	One activity is strongly favoured over another and its dominance is showed in practice
9	Extreme	Evidence of favouring one activity over another is of the highest degree possible of an affirmation
2, 4, 6, 8	Intermediate values	Used to represent compromises between the preferences in weights 1,3,5,7 and 9
Reciprocals	Opposites	Used for inverse comparisons

Moreover, the final weightings for the parameters are the normalized values of the eigenvectors that is associated with the maximum eigenvalues of the reciprocal matrix. The Consistency Ratio measures how far a matrix is away from consistency. A Consistency Ratio (CR) indicates the probability that the matrix ratings were randomly generated and when CR is less than or equal to the threshold 0.1 (Table 2) signifies an acceptable reciprocal matrix, while ratio over 0.1 implies that the matrix should be revised indicating inconsistent judgements and is given by the equation:

$$CR = {}^{CI}\!/_{RI}$$

where,

CI *the Consistency Index given by the equation:*

$$CI = {}^{(\lambda_{max} - n)}\!/_{(n - 1)}$$

where,

λ_{max} *the maximum eigenvalue (priority vector multiplied by each column total)*

n *the number of variables involved and*

RI *the Random Index (Table 1) for matrices which is based on the number of variables (n)*

Table 2: The values of the Random Index (RI) used to CR computation.

Matrix order	1	2	3	4	5	6	7	8	9	10	11	12	13	14	15
Random Index (RI)	0.00	0.00	0.58	0.90	1.12	1.24	1.32	1.41	1.51	1.49	1.52	1.54	1.56	1.58	1.59

3. Results and Discussion

3.1 Variables Selection

Slope (S)

The landslides usually occur as the surface slope increases due to the instability of certain rock formations to remain at their positions. Steeper slopes are more susceptible to landslides since high slope gradients are prone to slope failures, while flat areas are not vulnerable to landslide occurrences. Geomorphologically, the slope varies with high slopes (30°-55°) in the mountainous areas, moderate to steep slopes (10°-30°) in the hilly areas and gentle to moderate slope (0°-10°) in the plain. The slope map (Fig.3) of the Atalanti basin was reclassified into seven (7) classes varing from 0–5 to >45%.

Aspect (A)

This parameter (Fig.3) has been derived from the digital terrain model, paying particular attention to those areas that are windy and receive the highest rainfall amount, in this case, SW, W, NW and N directions (regulates the exposure to weather conditions, such as duration of sun exposure, rainfall intensity, moisture conservation, etc.). The slope direction plays a decisive role in the type of vegetation that develops, since it is heavily influenced by the amount of received solar energy. Consequently, SW slope direction is this which is favored by solar radiation, in relation to the North direction, in the development of vegetation and cultivation.

Curvature (C)

It has been derived from the digital terrain model taking into consideration that, depending on the relief curvature, it is facilitated or made difficult by the landslides' occurrences. The concave-negative values facilitate the occurrence of landslides as opposed to convex (positive) ones (Fig.3).

Elevation (E)

Naturally, high elevation areas have been assigned the highest rating, as landslide prone areas (Fig.3). Within the study area, the mountainous areas account only for 2.2% (>800 m) of the total area mainly at the Southern end of the basin (Mt. Chlomo). The semi-mountainous topographical zone accounts for 4.5% (600-800 m) while the flat areas account for 39.5% (0-200 m) mostly concerning the coastal areas. Also, the hilly and semi-hilly areas occupy almost 54% (200-600 m) of the basin.

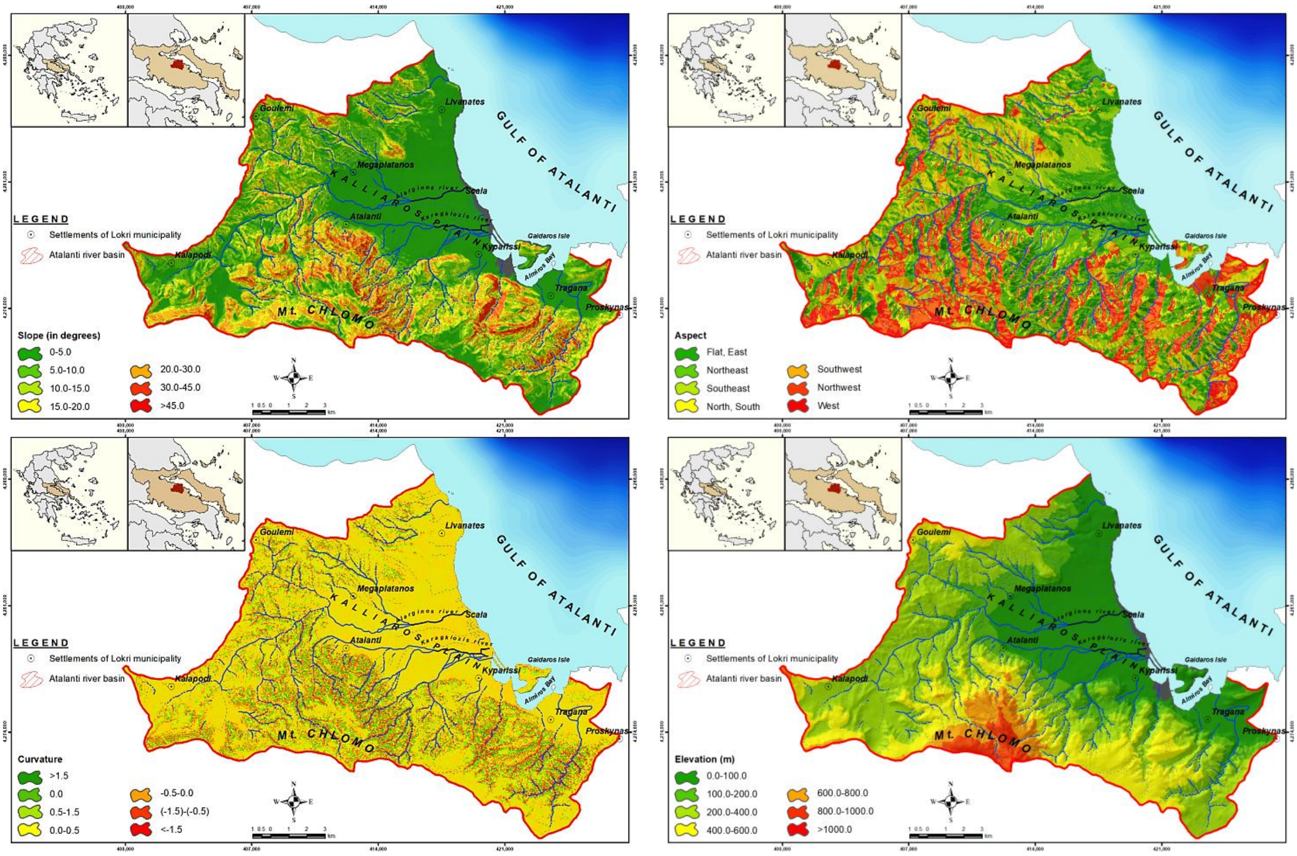

Fig.3: Thematic maps of basin's slope, aspect, curvature and elevation with classification.

Geology – Lithology (G)

Given that different lithological units exhibit different slope stability behavior, lithology plays a very significant role in landslides susceptibility zonation, since they are closely related to the lithological composition and materials' disintegration. The regional area is consisted of metamorhic-ultrabasic rocks of Paleozoic age such as shales and schists, of ophiolithic rocks (diabases, peridotites, serpentines) and flysch and of formations from Triassic to Createaceous age (e.g. dolomites and limestones) with large-scale faulting zones (WNW and NNE directions), fractures, fissures and cracks. Post-alpine mostly unconsolidated sediments such as sandstones, conglomerates, marls and alluvial deposits of Tertiary (Neogene-Pleiocene) and Quaternary age (Maratos et al., 1965) cover the Kalliaros plain. According to the geology-lithology, seven (7) classes were considered with flysch, schists and shales being attributed the lowest rate, marls the medium one and dolomites-limestones as well as the alluvial deposits with the lowest rate value because of their hardness the former and the low elevated occupied areas the latter (Fig.6).

Rainfall (R)

Heavy rainfalls are one of the main landslide-triggering factors. Both the rainfall intensity and precipitation itself in a given area, combined with other factors, affect the faster landslides occurrences. In the present essay, monthly precipitation data (Fig.4) of 51 years (1963-2014) from Atalanti rain gauge as well as mean annual precipitation data from 35 adjacent meteorological stations collected from the Hellenic National Meteorological Service (HNMS) and the Ministry of Environment and Energy were used to calculate the rainfall distribution and interpolated to create a continuous raster rainfall map within and around the study area (Fig.5). The values of this parameter were classified into seven classes between 450 mm and 1300 mm. As illustrated in Fig.6, the higher values were located in the hilly and mountainous parts of the study area whereas the lower ones in the flat relief (Kalliaros plain), as expected (Fig.6).

Land Use (LU)

Land use affects infiltration rate with forest and vegetated areas favoring infiltration, while urban, residential and pasture areas aggregating the overland flow due to the impervious cover which reduces infiltration capacity and increases runoff showing high susceptibility to landslideing. According to Corine Land Cover European programme (2012) the study area is covered by 13 discrete land use categories the most important of which are those of sclerophyllous vegetation (29.7%), non-irrigated arable land (20.5%) and complex cultivation patterns (11.7%), a relatively small percent by transitional woodland – shrub (9.7%) and land principally occupied by agriculture with significant areas of natural vegetation (6.9%) and finally, areas with mixed forest (2.3%), natural grasslands (1.4%) and discontinuous urban fabric (1.2%). In the Land Use map (Fig.6), seven (7) classes were identified, namely, urban/residential areas, forests, olive groves and vineyards, croplands, sclerophyllous vegetation, non-arable land and transitional lands. In many cases, vegetation favors the slope stability, contributing to the drainage of part of the water through the root system of the trees and limiting the corrosive action of the surface water. However, there are cases where the presence of vegetation can have negative consequences.

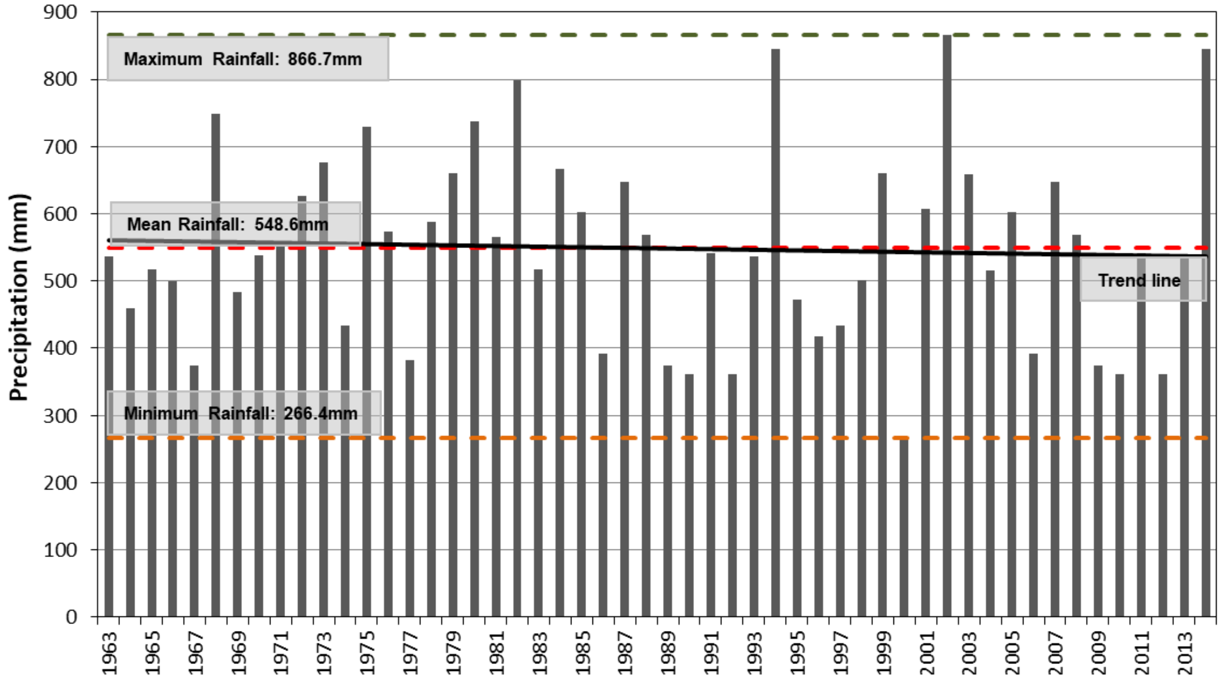

Fig.4: Mean monthly rainfall values in Atalanti meteorological station. The red dashed line shows the average precipitation value of the time series (1981-2014) and the green solid one the 12-month moving average.

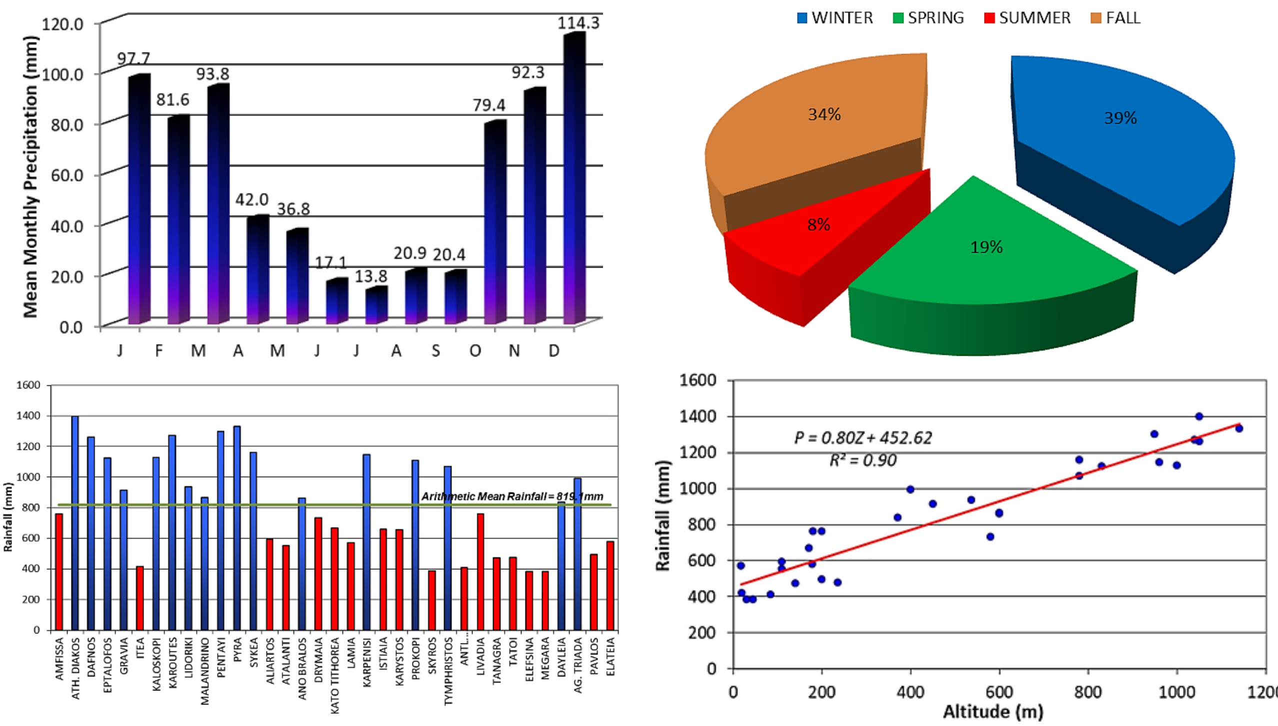

Fig.5: The over-annual precipitation for the entire time period (up-left), the rainfall seasonal distribution (up-right), the mean over-annual precipitation of the stations in the regional area (down-left) and the rain gradient equation for the regional area according to linear regression analysis (down-right).

Distance to Tectonics (T)

Whereas the study area is located in a tectonic active zone (Atalanti Fault Zone), the participation of the distance factor from the faults is considered necessary for further analysis. In order to investigate the landslides in relation to the distance from the tectonic elements, classe have been made per 100m equidistance (interval) with high distance from tectonics was ranked with the lowest rate value while this with low distance wase ranked with the highest rate value, as illustrated in Fig.6.

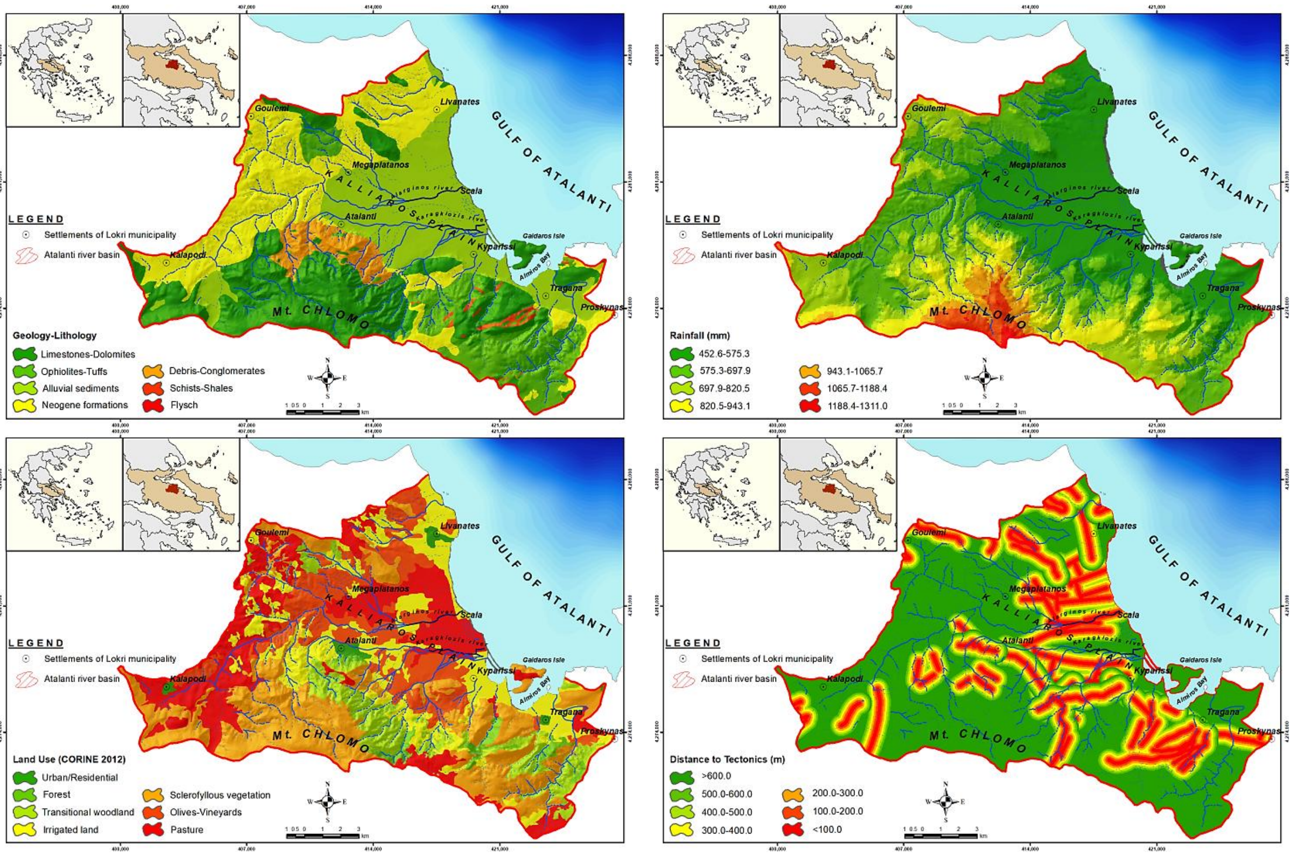

Fig.6: Thematic maps of geology, rainfall, land use and distance to tectonics with classification.

Distance to Drainage (D)

River erosion and surface runoff are one of the most important triggering factors, especially in areas with intense geomorphological relief and dense drainage network with deep valleys. The distance from surface runoff is therefore an important factor in characterizing vulnerable areas. The distance from river network plays an important role in defining the landslide areas. The role of a river decreases as the distance from river banks increases. For the study area, it appears that areas near the river network (<50 m) are highly landslide susceptible, while the effect of this parameter significantly decreases with no landslide phenomena in distance >500 m. The most affected areas during landslides are those nearby the river channels. The drainage network was reclassified in seven classes and areas with high distance from drainage were ranked with the lowest rate value while those with low drainage distance were ranked with the highest rate value, as illustrated in Fig.7.

Distance to Transportation (TR)

Road data have been derived from topographical maps of scale 1:50,000 with 50m equidistance zones (intervals). The road network is the result of anthropogenic interference in nature, which could potentially contribute to the reduction of slope stability and consequently the occurrence of adverse effects due to inappropriate construction and/or lack of rainwater drainage network (Fig.7).

Topographic Wetness Index (TWI)

The Topographic Wetness Index (TWI) combines the upstream contributing area per unit and slope and is mostly used to quantify topographic control on hydrological processes and distribute the soil moisture in a given area (Fig.7). The TWI is given by the equation:

$$\mathrm{TWI} = \ln\left({}^{\alpha}/_{tan\beta}\right)$$

where,

a   *the upslope contributing area (flow accumulation raster map for the corresponding DEM)*
tanβ   *the slope angle (the slope raster map in degrees for the corresponding DEM)*

High values represent drainage depressions (lowlands with low slope gradient) with wet ground while low ones represent crests and ridges (highlands with high slope gradient). The higher value of TWI the more susceptible areas to landslides.

Stream Power Index (SPI)

The Stream Power Index (SPI) is a measure of the erosive power of the water flowing at the surface. SPI is calculated based upon slope angle and upstream drainage area. SPI approximates locations where gullies might be more likely to form on the landscape. Stream Power Index (SPI) takes into consideration both a local slope geometry and site location combining data on slope gradient and basin area, as follows:

$$\mathrm{SPI} = \ln(a \times \tan\beta)$$

where,

a *the upstream drainage area (flow accumulation raster map for the corresponding DEM)*

tanβ *the slope angle (the slope raster map in degrees for the corresponding DEM)*

The higher value of SPI the more prone areas to landslides (Fig.7).

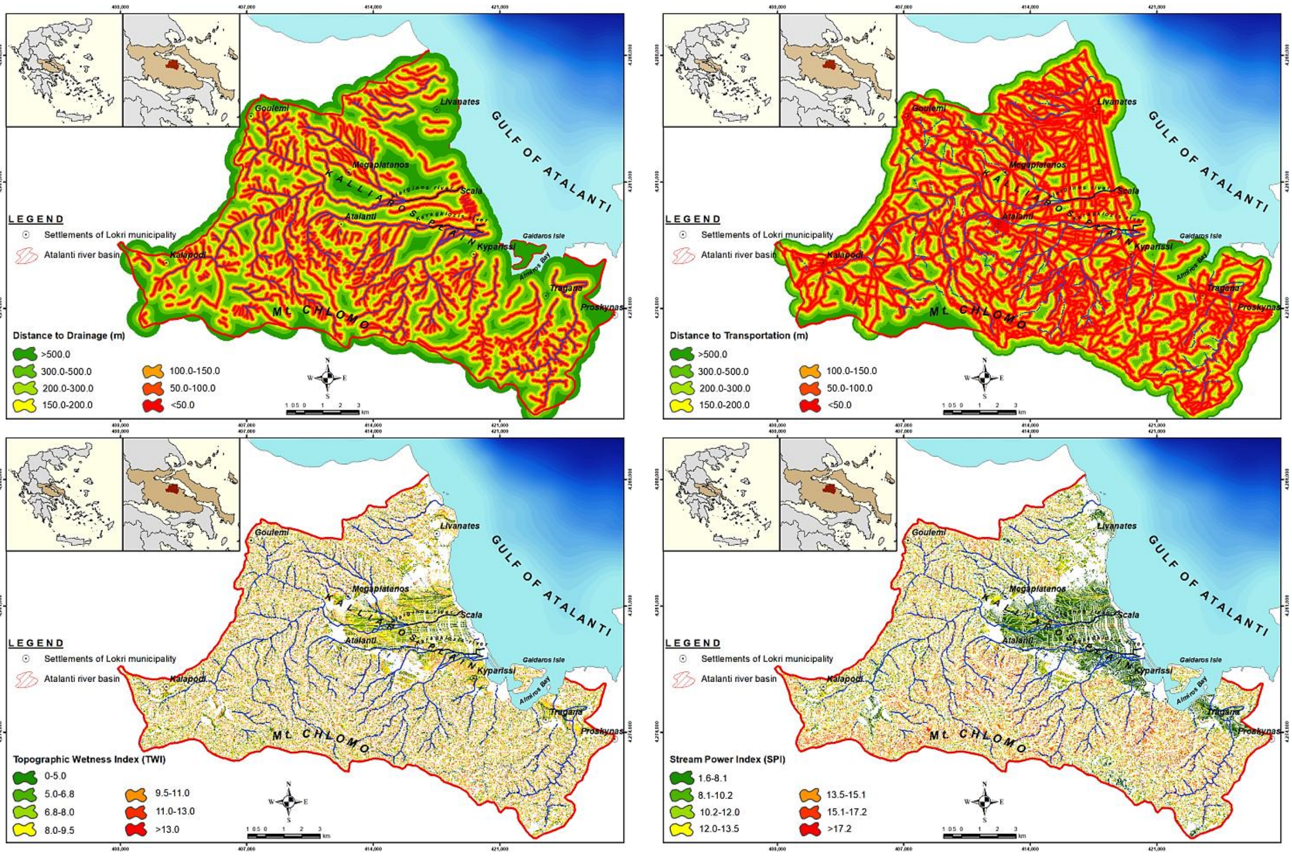

Fig.7: Thematic maps of distance to drainage and transportation, topographic wetness and stream power indices with classification.

3.2 Results' Evaluation – Validation

According to AHP method the rating score of each variable ranged from 1 to 10 indicating the classes from "Very Low" to "Very High". Then, each variable was assigned to a unique weight based on expert judgement, decision-maker's preference and scientific references. The total weight was resulted by the sum up of the weight and ranking multiplication. After following the same procedure for all the aforementioned criteria, the gross weight of the total one is shown in Table 3.

Table 3: Variables weights' assignment to landslide susceptibility based on AHP method.

Variables	**Geology – Lithology**	**Distance to Tectonics**	**Slope**	**Aspect**	**Rainfall**	**Elevation**	**Land Use**	**Distance to Transportation**	**Distance to Drainage**	**Curvature**	**Topographic Wetness Index**	**Stream Power Index**	**Weight (by Eigen)**
Geology – Lithology (G)	**1**	2	1/3	3	1/2	7	3	2	3	3	4	5	***0.116***
Distance to Tectonics (T)	1/2	**1**	1/3	2	1/2	6	2	1	1	7	2	3	***0.091***
Slope (S)	3	3	**1**	5	2	9	5	3	4	2	6	7	***0.205***
Aspect (A)	1/3	1/2	1/5	**1**	1/5	6	1/2	1/4	1/5	3	1/3	1/4	***0.039***

Variables	**Geology – Lithology**	**Distance to Tectonics**	**Slope**	**Aspect**	**Rainfall**	**Elevation**	**Land Use**	**Distance to Transportation**	**Distance to Drainage**	**Curvature**	**Topographic Wetness Index**	**Stream Power Index**	**Weight (by Eigen)**
Rainfall (R)	2	2	1/2	5	**1**	7	4	3	2	4	6	8	***0.163***
Elevation (E)	1/7	1/6	1/9	1/6	1/7	**1**	1/5	1/8	1/8	1/5	1/2	1/3	***0.013***
Land use (LU)	1/3	1/2	1/5	2	1/4	5	**1**	1/3	1/3	1/2	1/4	1/4	***0.034***
Distance to Transportation (TR)	1/2	1	1/3	4	1/3	8	3	**1**	1/2	1/4	1/2	1/3	***0.059***
Distance to Drainage (D)	1/3	1	1/4	5	1/2	8	3	2	**1**	1/8	1/5	1/3	***0.065***
Curvature (C)	1/3	1/7	1/2	1/3	1/4	5	2	4	8	**1**	2	3	***0.088***
Topographic Wetness Index (TWI)	1/4	1/2	1/6	3	1/6	2	4	2	5	1/2	**1**	3	***0.068***
Stream Power Index (SPI)	1/5	1/3	1/7	4	1/8	3	4	3	3	1/3	1/3	**1**	***0.059***
												Consistency Ratio	***CR = 0.067***

Validation – verification is a very important process for any model as it provides the ability to acquire knowledge about the predictive model values. All the citeria used quantitative (numeric) parameters except for the factors "aspect", "geology" and "land use" (descriptive). In the case of the non-numeric factors, classification depends mainly on the influence of the factor on the recharging landslide process (Table 4). These criteria all combined based on their proportions were resulted in the landslide susceptibility map shown in Fig.8. The basin's slope and the rainfall were assigned with the highest weights followed by the "geology" and the "distance to tectonics". On the contrary, the "land use", the "elevation" as we;; as the "aspect" were assigned with the lowest weights. As illustrated in Fig.8 the classes "Moderate to High", "High" and "Very High" cover a surface of 17.4% or 43.3 km^2 of the total basin. Also, according to the same map, the above categories of landslide susceptibility are mainly found in the central and southern parts of the study area (semi-mountainous, mountainous sections with steep slopes), as well as in the southeast (south of the settlements of Kyparissi and Tragana). On the contrary, the other classes cover mostly lower slope gradient areas (82.6% or 206.3 km^2). Finally, as shown in Fig.8 the landslide areas based on historical records fall within the classes "High" and "Very High" validating the reliability of the applied methodology. Overlaying the map with the recordings of landslide events has shown that about 81.8% of those are found in zones of high and very high susceptibility classes. These results show a model with satisfactory precision within the work scale.

In conclusion, the use of spatial analysis methods based on geoinformatics is a very effective tool of risk management of natural disasters on a regional scale. This methodology for mapping susceptibility to landslides included the creation of thematic layers, the development of an appropriate graphical, the numerical distribution, the integration of spatial data and finally, the enhancement of results in relation to the recorded landslides. The produced maps are intended to assist in decision-making and if areas of high susceptibility can not be avoided, all necessary precautions should be taken to minimize the likelihood of landslides. It is clearly obvious that the weighting of the different criteria significantly affects the results of the overall evaluation since the rating for each criterion may differ from scientist to scientist. To sum up, the landslide map produced is regarded as satisfactory and can be used for a first overview and approach to areas that require further study, control and monitoring. As the sensitivity of the proposed methodology is based on the choice of parameters that affect their landslide hazard and calibration, it is considered necessary to further study and combine other methodologies (graphical spatial analysis and statistics) to better simulate the landslide susceptibility of the area study.

Table 4: Variables contributing to landslide susceptibility assessment.

Variables/Criteria	Range	Classes	Ranking-R_i	Weight-w_i
Slope (degrees) (S)	0.0-5.0	Very Low	1.0	0.205 (20.5%)
	5.0-10.0	Low	2.5	
	10.0-15.0	Low to Moderate	4.0	
	15.0-20.0	Moderate	5.5	
	20.0-30.0	Moderate to High	7.0	
	30.0-45.0	High	8.5	
	>45.0	Very High	10.0	
Aspect (A)	Flat, East	Very Low	1.0	0.039 (3.9%)
	Northeast	Low	2.5	
	Southeast	Low to Moderate	4.0	
	North, South	Moderate	5.5	
	Southwest	Moderate to High	7.0	
	Northwest	High	8.5	
	West	Very High	10.0	
Curvature (C)	>1.5	Very Low	1.0	0.088 (8.8%)
	0.0	Low	2.5	
	0.5-1.5	Low to Moderate	4.0	
	0.0-0.5	Moderate	5.5	
	-0.5-0.0	Moderate to High	7.0	

Variables/Criteria	Range	Classes	Ranking-R_i	Weight-w_i
	(-1.5)-(-0.5)	High	8.5	
	<-1.5	Very High	10.0	
Elevation (m) (E)	0.0-100.0	Very Low	1.0	0.013 (1.3%)
	100.0-200.0	Low	2.5	
	200.0-400.0	Low to Moderate	4.0	
	400.0-600.0	Moderate	5.5	
	600.0-800.0	Moderate to High	7.0	
	800.0-1000.0	High	8.5	
	>1000.0	Very High	10.0	
Geology – Lithology (G)	Limestones-Dolom.	Very Low	1.0	0.116 (11.6%)
	Ophiolites-Tuffs	Low	2.5	
	Alluvial sediments	Low to Moderate	4.0	
	Neogene formations	Moderate	5.5	
	Debris-Conglom.	Moderate to High	7.0	
	Schists-Shales	High	8.5	
	Flysch	Very High	10.0	
Rainfall (R)	452.6-575.3	Very Low	1.0	0.163 (16.3%)
	575.3-697.9	Low	2.5	
	697.9-820.5	Low to Moderate	4.0	
	820.5-943.1	Moderate	5.5	
	943.1-1065.7	Moderate to High	7.0	
	1065.7-1188.4	High	8.5	
	1188.4-1311.0	Very High	10.0	
Land Use (LU)	Urban / Residential	Very Low	1.0	0.034 (3.4%)
	Forest	Low	2.5	
	Transitional Woodland	Low to Moderate	4.0	
	Irrigated land	Moderate	5.5	
	Sclerofyllous Vegetation	Moderate to High	7.0	
	Olives / Vineyards	High	8.5	
	Pasture	Very High	10.0	
Distance to Tectonics (m) (T)	>600.0	Very Low	1.0	0.091 (9.1%)
	500.0-600.0	Low	2.5	
	400.0-500.0	Low to Moderate	4.0	
	300.0-400.0	Moderate	5.5	
	200.0-300.0	Moderate to High	7.0	
	100.0-200.0	High	8.5	
	<100.0	Very High	10.0	
Distance to Drainage (m) (D)	>500.0	Very Low	1.0	0.065 (6.5%)
	300.0-500.0	Low	2.5	
	200.0-300.0	Low to Moderate	4.0	
	150.0-200.0	Moderate	5.5	
	100.0-150.0	Moderate to High	7.0	
	50.0-100.0	High	8.5	
	<50.0	Very High	10.0	
Distance to Transportation (m) (TR)	>500.0	Very Low	1.0	0.059 (5.9%)
	300.0-500.0	Low	2.5	
	200.0-300.0	Low to Moderate	4.0	
	150.0-200.0	Moderate	5.5	
	100.0-150.0	Moderate to High	7.0	
	50.0-100.0	High	8.5	
	<50.0	Very High	10.0	
TWI	0-5.0	Very Low	1.0	0.068 (6.8%)
	5.0-6.8	Low	2.5	
	6.8-8.0	Low to Moderate	4.0	
	8.0-9.5	Moderate	5.5	
	9.5-11.0	Moderate to High	7.0	
	11.0-13.0	High	8.5	
	13.0-20.0	Very High	10.0	
SPI	1.6-8.1	Very Low	1.0	0.059 (5.9%)
	8.1-10.2	Low	2.5	
	10.2-12.0	Low to Moderate	4.0	
	12.0-13.5	Moderate	5.5	
	13.5-15.1	Moderate to High	7.0	
	15.1-17.2	High	8.5	
	>17.2	Very High	10.0	
Total	-	-	-	**1.0 (100.0%)**

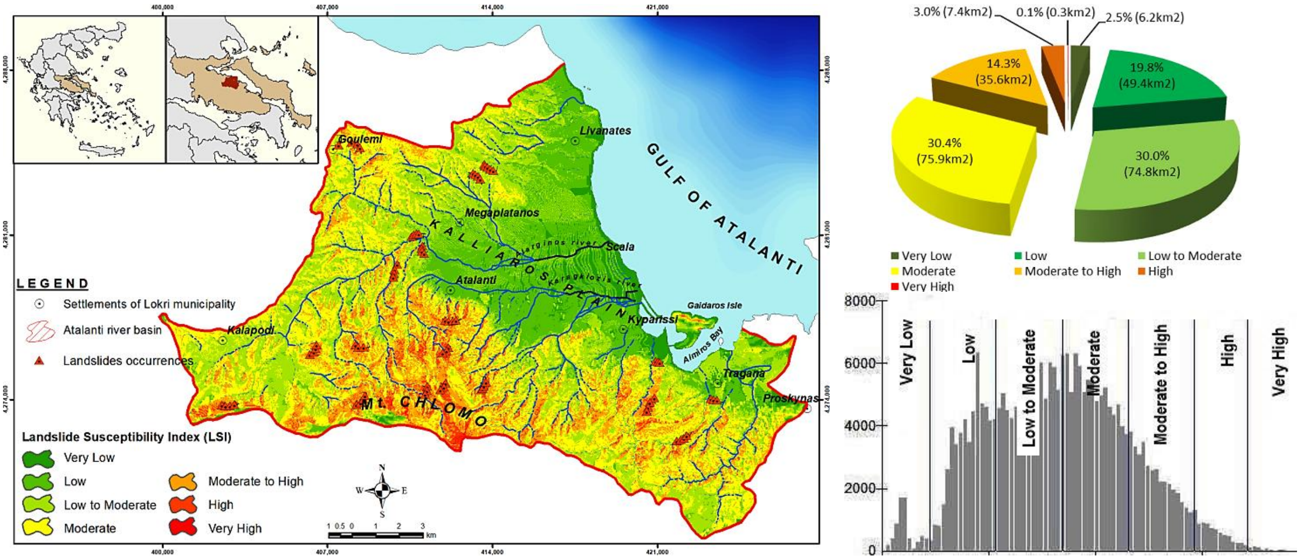

Fig.8: Landslide susceptibility map based on AHP method (left) and classes' surface distribution percentage (right).

3.3 Sensitivity Analysis

One way of analyzing the sensitivity analysis of a model is by varying the weight factor of the strongest factor by a small percentage (+5%), with the simultaneous inverse differentiation of the second stronger factor (-5%), so that the final sum of the coefficients be the same as the original one. Thereafter, this process can be repeated for as many modification values as decided. The values to be calculated for each case of modifying the model are the deviations from the original and consequently useful conclusions can be drawn as to the sensitivity (or not) of the result to these minor changes. In the present study four sensitivity analysis scenarios were selected. In the first sensitivity scenario, the coefficient of the basin's slope was increased by 0.05 and the coefficient of the second strongest variable, which is the rainfall, was decreased by 0.05 while the second scenario is the opposite. In the third scenario, the coefficient of the slope was increased again by 0.05 and the coefficient of the third most powerful factor, geology - lithology, was reduced by 0.05 while the fourth scenario is the opposite. The weighting ratios of the remaining variables for each sensitivity scenario remained unchanged.

In the table 5 and as illustrated in Fig.9, the quantitative comparison of the sensitivity analysis scenarios with the initial result of the model is presented. The values refer to the percentage (%) distribution and the percentage difference of the areas corresponding to each class relative to the original model. In the sensitivity analysis scenarios of the model, the deviations that appear were small and therefore the model is considered stable. In conclusion, multicriteria analysis using Analytical Hierarchy Process is a useful research tool in spatial decision making models. The AHP technique has a wide range of applications with very satisfactory results and is a structured, documented, self-controlled and relatively easy to apply technique. Finally, the ability of the method to combine quantitative and qualitative criteria with spatial differentiation makes it suitable for the analysis of complex geographic phenomena and problems, while its application to GIS environment in multi-criteria analysis with weighted cartographic overlay makes it a powerful analytical tool.

Table 5: Areal distribution percentage (%) in each class and difference between the applied model and each hypothetic scenario.

Classes	Model	Scen-1	Differ-1	Scen-2	Differ-2	Scen-3	Differ-3	Scen-4	Differ-4
Very Low	2.5	1.7	*-0.8*	2.7	*0.2*	2.3	*-0.2*	2.8	*0.3*
Low	19.7	19.1	*-0.6*	20.2	*0.5*	19.1	*-0.6*	20.4	*0.7*
Low to Moderate	30.0	29.2	*-0.8*	30.8	*0.8*	29.0	*-1.0*	30.2	*0.2*
Moderate	30.4	30.6	*0.2*	29.2	*-1.2*	30.5	*0.1*	30.3	*-0.1*
Moderate to High	14.3	14.8	*0.5*	13.8	*-0.5*	14.8	*0.5*	13.5	*-0.8*
High	3.0	3.5	*0.5*	3.1	*0.1*	3.7	*0.7*	2.6	*-0.4*
Very High	0.1	1.1	*1.0*	0.2	*0.1*	0.6	*0.5*	0.2	*0.1*

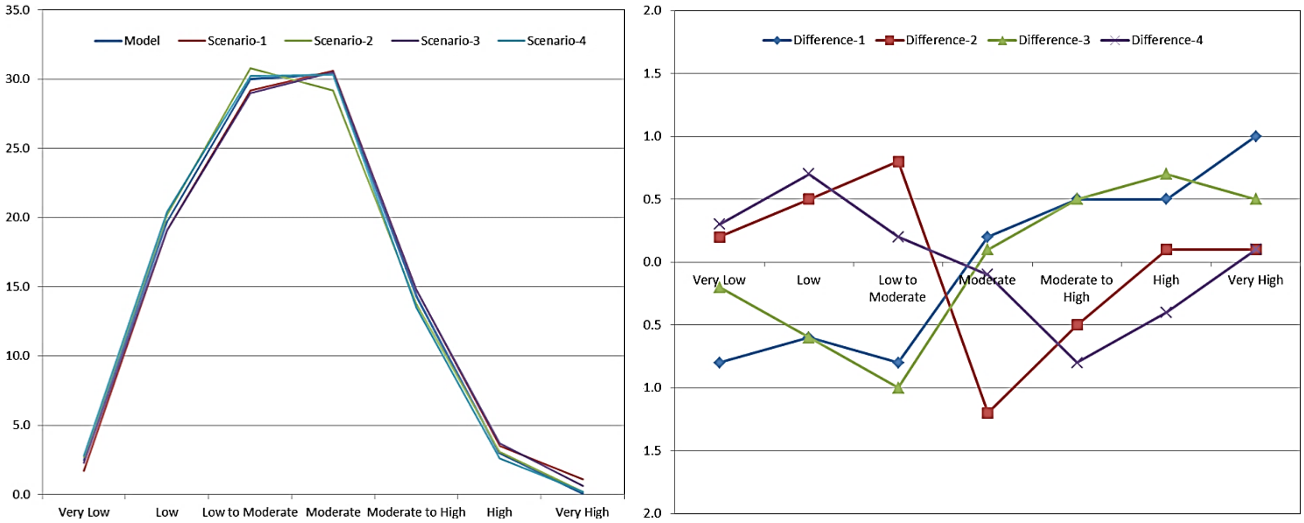

Fig.9: Graphical presentation for the surface distribution percentage (left) and the difference between the applied model and each hypothetic scenario (right).

4. Conclusions

This paper presented an approach to implement a semi-quantitative analysis of spatio-temporal landslide occurrences in the Atalanti area in central Greece. Based on landslide causative factors and a slope failure inventory, a susceptibility map was calculated by a GIS-based AHP method which ranked areas according to their probability to produce slope failures. In this research twelve factors were investigated to map the landslide susceptibility. Of those, four factors including slope, rainfall, geology and distance to tectonics were considered to be the main causative-triggering landsides factors. Based on the results, a large area in the district consisted of moderate and low to moderate landslides prone susceptibility categories. It was concluded that AHP model pointed out the interrelation between the occurrence of landslides and theirs causative-instability factors. Hence, it may be inferred that the map correlated satisfactorily with existing field conditions. As the final conclusion, the results in this study demonstrated that the proposed integration approach could be used for preliminary landslide studies, hazard mapping and other geo-environmental problems as it is capable of producing accurate assessments of landslide susceptibility that are useful for hazard prevention management and decision making. As the main outcome of this work, a landslide susceptibility map was finally produced and validated. Up to 3% of the whole watershed was assigned to the “high” and “Very High” susceptibility classes, revealing the geographical distribution of the areas most prone to landslide occurrences. A Weighted Linear combination method to determine the landslide susceptible zones was applied. The comparison of the landslide hazard map with the actual landslide activity distribution map has shown that almost 82% of the landslides lie within the maximum hazard zone. Finally, use of GIS was found immensely important for thematic data layer generation and for their spatial data analysis, which involved complex operations maximizing the functionality of GIS environment and producing quite accurate landslide susceptibility map.

Acknowledgments

The authors wish to express their thanks to the Hellenic Military Geographical Service (HMGS) for the topographical maps obtained as well as the Hellenic National Meteorological Service (HNMS) and the Ministry of Environment and Energy for the meteorological stations’ precipitation dataset of the regional area. Also, many thanks to the Institute of Geology and Mineral Exploration (IGME) for the given landslide inventory database.

Conflict of Interests

The authors confirm that there is no conflict of interests.

References

Atkinson, P., Massari, R. (1998). Generalized linear modelling of susceptibility to landsliding in the central Apennines, Italy. Computers & Geosciences, 24, 373-385.

Bathrellos, G., Kalivas, D., Skilodimou, H. (2009). GIS-based landslide susceptibility mapping models applied to natural and urban planning in Trikala, Central Greece. Estudios Geologicos, pp.49-65.

Carrara, A. (1983). Multivariate models for landslide hazard evaluation. Mathmatical Geology, 15(3), pp.403-427.

Carrara, A., Cardinali, M., Detti, R., Guzzetti, F., Pasqui, V., Reichenbach, P., (1991). GIS techniques and statistical models in evaluating landslide hazard, Earth Surface Processes and Landforms, 16, pp.427-445.

Carrara, A., Guzzetti, F., Cardinali, M., Reichenbach, P. (1999). Use of GIS technology in the prediction and monitoring of landslide hazard. Natural Hazards, 20, pp.117-135.

Carrara, A., Giovanni, C., Frattini, P. (2003). Geomorphological and historical data in assessing landslide hazard. Earth Surface Processes and Landforms, 28, p.545.

Carrara, A., Pike, J. (2008). GIS technology and models for assessing landslide hazard and risk. Geomorphology, 94, pp.257-260.
Chalkias, Ch., Ferentinou, M., Polykretis, Ch. (2014). GIS-Based Landslide Susceptibility Mapping on the Peloponnese Peninsula, Greece. Geosciences, 4, pp.176-190.
Chau, K., Sze, Y., Fung, M., Wong, W., Fong, E., Chan, L. (2004). Landslide hazard analysis for HongKong using landslide inventory and GIS. Computers & Geosciences, 30, pp.429-443.
Chung, C., Fabbri, G. (2003). Validation of spatial prediction models for landslide hazard mapping. Natural Hazards, 30, pp.451-472.
Dai, F., Lee, F., Li, J., Xu, W. (2001). Assessment of landslide susceptibility on the natural terrain of Lantau Island, Hong Kong. Environmental Geology, 40, pp.381-391.
Ferentinou, M., Chalkias, Ch., Sakellariou, M. (2010). Landslide susceptibility mapping in national scale and preliminary risk analysis applying computational methods in a GIS environment, 9th Panellenic Conference of Geography, pp.682-689.
Gupta, R., Joshi, B. (1990). Landslide hazard zoning using the GIS approach—a case-study from the Ramganga Catchment, Himalayas. Engineering Geology, 28, pp.119-131.
Kritikos, T., Davies, T. (2011). GIS-based multi-criteria decision analysis for landslide susceptibility mapping at northern Evia, Greece. Zeitschrift der Deutschen Gesellschaft für Geowissenschaften, 162, pp.421-434.
Kumar, M., Annadurai, R. (2013). Mapping of Landslide Susceptibility Using Geospatial Technique – A Case Study in Kothagiri Region, Western Ghats, Tamil Nadu, India. International Journal of Engineering Research & Technology (IJERT), vol.2, issue 12.
Ladas, I., Fountoulis, I., Mariolakos I. (2007). Using GIS & multicriteria decision analysis in landslide susceptibility mapping. A case study in Messinia prefecture area (SW Peloponnesus, Greece). Bulletin of the Geological Society of Greece vol.XXXX, Proceedings of the 11th International Congress, Athens.
Lappas, I. 2018. Applied hydrogeological research in coastal aquifers. Case study of the coastal part of Atalanti region, Prefecture of Fthiotida. PhD Thesis Dissertation, School of Mining and Metallurgical Engineering, National and Technical University of Athens, p.487.
Mancini, F., Ceppi, C., Ritrovato, G. (2010). GIS and statistical analysis for landslide susceptibility mapping in the Daunia area, Italy. Natural Hazards and Earth System Sciences, pp.1851-1864.
Maratos, G., Rigopoulos, K., Athanasiou, A. (1965). Geological maps of Atalanti and Livanates sheets, scale 1:50.000, Institute of Subsurface Geological Research.
Marinoni, O. (2004): Implementation of the analytical hierarchy process with VBA in ArcGIS. Computers and Geosciences, 30, 6, pp.637-646.
Papadakis, M., Karimalis, A. (2017). Producing a Landslide Susceptibility Map through the Use of Analytic Hierarchical Process in Finikas Watershed, North Peloponnese, Greece. American Journal of Geographic Information System, 6, pp.14-22.
Polykretis, C., Ferentinou, M., Chalkias, C. (2014). A comparative study of landslide susceptibility mapping using landslide susceptibility index and artificial neural networks in the Krios River and Krathis River catchments (northern Peloponnesus, Greece). Bull. Eng. Geol. Environ.
Rozos, D., Bathrellos, D., Skilodimou, D. (2010). Landslide susceptibility mapping of the northeastern part of Achaia prefecture using analytical hierarchical process and GIS techniques. Bulletin of the Geological Society of Greece, Proceedings of the 12th International Congress, Patra.
Rozos, D., Bathrellos, G., Skillodimou, H. (2011). Comparison of the implementation of rock engineering system and analytic hierarchy process methods, upon landslide susceptibility mapping, using GIS: a case study from the Eastern Achaia County of Peloponnesus, Greece. Environmental Earth Science, 63, pp.49-63.
Saaty, T. 1977. A scaling method for priorities in hierarchical structures. Journal of Mathematical Psychology, 15 (3), pp.234-281.
Saaty, T. (1980). The Analytic Hierarchy Process. McGraw-Hill, New York, pp.20-25.
Saaty, T. (1990). How to Make a Decision: The Analytic Hierarchy Process, European Journal of Operational Research, 48, 1, pp.9-26.
Saaty, L., Vargas, G. (1991). Prediction, Projection and Forecasting. Kluwer Academic Publishers, Dordrecht, p.251.
Saaty, T. (2000). Fundamentals of Decision Making and Priority Theory with the Analytic Hierarchy Process. 2nd Edn., RWS Publications, Pittsburgh, USA.
Sarkar, S., Kanungo, D. (2004). An Integrated Approach for Landslide Susceptibility Mapping Using Remote Sensing and GIS. Photogrammetric Engineering & Remote Sensing, vol.70, No.5, pp.617–625.
Shahabi, H., Hashim, M. (2015). Landslide susceptibility mapping using GIS-based statistical models and Remote sensing data in tropical environment. Scientific Reports, pp.1-15.
Tazik, E., Jahantab, Z., Bakhtiari, M., Rezaei, A., Alavipanah, S. (2014). Landslide susceptibility mapping by combining the three methods Fuzzy Logic, Frequency Ratio and Analytical Hierarchy Process in Dozain basin. The International Archives of the Photogrammetry, Remote Sensing and Spatial Information Sciences, vol.XL-2/W3, Tehran, Iran.
Tsangaratos, P., Rozos, D. (2013). Producing landslide susceptibility maps by applying expert knowledge in a GIS – based environment. Proceedings of the 13th International Congress, Chania.

